Received: 16 December 2021 | Revised: 14 February 2022 | Accepted: 25 February 2022

DOI: 10.1002/hyp.14532

SCIENTIFIC BRIEFING

HP TODAY WILEY

Estimates of water partitioning in complex urban landscapes with isotope-aided ecohydrological modelling

Mikael Gillefalk[1,2] | Doerthe Tetzlaff[2,3] | Christian Marx[1,2] | Aaron Smith[2] | Fred Meier[4] | Reinhard Hinkelmann[1] | Chris Soulsby[1,2,5]

[1]Chair of Water Resources Management and Modeling of Hydrosystems, Technische Universität Berlin, Berlin, Germany

[2]Department of Ecohydrology, Leibniz Institute of Freshwater Ecology and Inland Fisheries, Berlin, Germany

[3]Department of Geography, Humboldt University of Berlin, Berlin, Germany

[4]Chair of Climatology, Technische Universität Berlin, Berlin, Germany

[5]Northern Rivers Institute, University of Aberdeen, St. Mary's Building, Kings College, Old Aberdeen, Scotland

Correspondence
Mikael Gillefalk, Chair of Water Resources Management and Modeling of Hydrosystems, Technische Universität Berlin, Berlin, Germany.
Email: mikael.gillefalk@tu-berlin.de

Funding information
Berlin University Alliance / Einstein Stiftung Berlin, Climate and Water under Change; Deutsche Forschungsgemeinschaft, Grant/Award Number: Urban Water Interfaces (GRK2032/2); Einstein Stiftung Berlin, Grant/Award Number: MOSAIC (EVF-2018-425); Leverhulme Trust, Grant/Award Number: ISOLAND (RPG-2018-425); Urban Climate Observatory (UCO) Berlin, Grant/Award Number: 01LP1602

Abstract

Urban green space is increasingly viewed as essential infrastructure to build resilience to climate change by retaining water in the city landscape and balancing ecohydrological partitioning into evapotranspiration for cooling and groundwater recharge. Quantifying how different vegetation types affect water partitioning is essential for future management, but paucity of data and the complex heterogeneity of urban areas make water balance estimates challenging. Here, we provide a preliminary assessment of water partitioning from different sized patches of trees and grass as well as from sealed surfaces. To do this, we used limited field observations together with an advanced, process-based tracer-aided ecohydrological model at a meso-scale (5 km^2) in central Berlin, Germany. Transpiration was the dominant green water flux accounting for over 50% of evapotranspiration in the modelled area. Green water fluxes were in general greater from trees compared with grass, but grass in large parks transpired more water compared with grass in small parks that were intensively used for recreation. Interception evaporation was larger for trees compared with grass, but soil water evaporation was greater for grass compared with trees. We also show that evapotranspiration from tree-covered areas comprise almost 80% of the total evapotranspiration from the whole model domain while making up less than 30% of the surface cover. The results form an important stepping-stone towards further upscaling over larger areas and highlights the importance of continuous high-resolution hydrological measurements in the urban landscape, as well as the need for improvements to ecohydrological models to capture important urban processes.

KEYWORDS
ecohydrological modelling, ecohydrology, isotopes, sealed surfaces, tracers, urban green spaces, urban hydrology, water partitioning

1 | INTRODUCTION

In the context of water management in urban areas, green spaces play an increasingly crucial role by helping to retain water in the landscape. Such green 'infrastructure' has the potential to combat the urban heat island effect (Peng et al., 2012), via cooling and latent heat transfers (Bowler et al., 2010), as well as enabling groundwater recharge (Golden & Hoghooghi, 2018) rather than direct runoff to storm drains.

However, these two effects are potentially competing and need careful evaluation depending on the specific geographical setting and local priorities. Whatever the goal of urban policy is, local knowledge and quantification of green water fluxes and partitioning into interception, transpiration, soil evaporation and recharge is urgently needed. Traditionally, modelling studies on water in an urban context have focussed on drainage and flooding (e.g., Cao et al., 2020; Zhou et al., 2017). Until recently, very few studies attempted to improve process-based estimates of ecohydrological fluxes from urban green spaces (e.g., Cristiano et al., 2020; Meili et al., 2020). Consequently, process-based models for green water flux estimates are crucial, which has been specifically highlighted as a priority for improvement by the research community (Tague et al., 2020).

However, there are specific challenges which impede progress: any spatially distributed, process-based model in urban hydrology is confronted with the urban fabric, which is highly heterogeneous and contrasting in character with a mix of built environment and green space. It has a mosaic of patches of different sizes, shapes, orientations and edge effects. These different patches have high variability in permeability which changes the distribution of water fluxes and storage across the urban landscape. Additionally, more complex controls like heat storage, shading, wind 'funnelling' and irrigation influence the hydrological cycle in cities. On top of this, distributed monitoring is very difficult in urban areas due to the high heterogeneity, accessibility and risk of vandalism on public lands, and permissions needed on private land. Hence, the incorporation of field data into more robust hydrological models is much less advanced than in more rural environments and experimental catchments.

The use of stable water isotopes as tools to better constrain models of urban water flow paths and flux estimates is still quite recent (e.g., Ehleringer et al., 2016). Stable isotopes, such as δ^2H and $\delta^{18}O$, are tracers of precipitation partitioning, evaporation fractionation and mixing in the subsurface. By integrating stable isotopes into ecohydrological models, green water fluxes can be resolved and better constrained, as recently shown with the process-based tracer-aided ecohydrological model EcH_2O-iso (Kuppel et al., 2018). In urban settings the use of the model has so far been limited to small scales at an intensively monitored site (Gillefalk et al., 2021). In that case stable isotopes in soil water, together with soil moisture content and sap flow data were successfully simulated to quantify ecohydrological fluxes, estimate water ages and explore the impact of sealed surfaces at a plot scale.

Given the urgent need to improve process-based estimates of water partitioning in urban green space, here, in a 'proof of concept' study, we attempted to upscale the application of EcH_2O-iso model domain (from <0.01 to >5 km^2). This study used a similar approach as Gillefalk et al. (2021) but with more limited, non-continuous data for a mosaic of green space which is more typical of a larger urban area. The study also seeks to incorporate a first approximation of losses from sealed surfaces. The specific aims are to: (a) apply a tracer aided ecohydrological model with spatially distributed soil moisture and soil water isotope data as calibration constraints over larger complex cityscapes, (b) compare water balance components from the complex mosaic of an urban landscape containing larger areas of dense vegetation (grass and trees), sparsely vegetated smaller areas (grass and trees) as well as almost fully sealed areas and (c) provide an integrated estimate of evapotranspiration (ET) fluxes and resolved component parts over the model domain.

2 | METHODS

2.1 | Study area description

The study was located in a ~ 5 km^2 area in central Berlin, Germany (Figure 1). It encompasses a range of different sized green spaces, typical for urban areas, as well as large areas of sealed surfaces (e.g., roofs, roads, courtyards etc.). Central to this study are three parks: Volkspark Humboldthain (Humboldthain), Brunnenplatz and Volkspark am Weinberg (Weinberg). Humboldthain is the largest, being 29 ha, Brunnenplatz and Weinberg are smaller, 3.3 and 4.3 ha, respectively. All parks have a mixture of both grassland and trees and all of them have a high degree of usage, especially in summer.

The climate in Berlin is transitional between a temperate oceanic and a warm-summer humid continental climate (Köppen classification: Dfb and Cfb; Beck et al., 2018). The long-term mean annual temperature is 9.7°C and precipitation is 591 mm (DWD, 2020). The precipitation is almost equally distributed over summer and winter, though the summer is dominated by sporadic, intense, convective rainfall and the winter by more frequent, lower intensity, prolonged frontal rain.

2.2 | Available data

Inputs to drive the EcH_2O-iso application were hydroclimate data with daily resolution: shortwave radiation, longwave radiation, precipitation, air temperature, humidity and wind speed. The radiation, humidity and wind speed were measured by an eddy flux tower for the period 1 June 2018 until 27 November 2020 at a site ~10 km SW of the study area, at the Urban Climate Observatory in Steglitz. For the period 1 Jan 2018 until 31 May 2018, data from an eddy flux tower located ~6 km SW of the study area were used, at the TU Berlin Campus Charlottenburg. The data had few missing values (<0.5%) during the calibration period. The precipitation was measured by the German Weather Service (DWD) at the Berlin Tegel Airport, ~6 km NW of the study area. The distance to the study area was deemed small enough to not have a significant impact on the modelling study. The climate input was applied uniformly over the study area.

Precipitation for analysis of stable isotopes was sampled daily from two sites beginning in August 2018: at the Leibniz Institute of Freshwater Ecology and Inland Fisheries location in Berlin-Friedrichshagen and from the Steglitz Urban Ecohydrological Observatory in Berlin-Steglitz (Figures 2 and 3).

Soil water content (SWC) was measured in Brunnenplatz (three grass and two tree plot sites), in Humboldthain (two grass and four

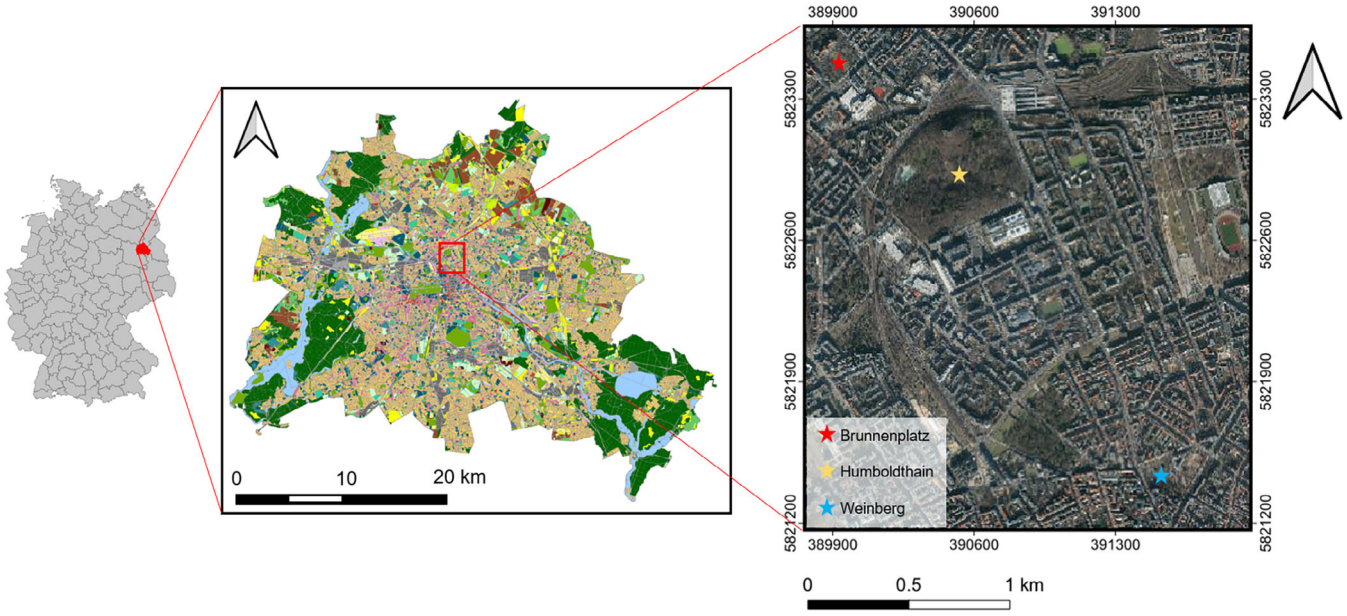

FIGURE 1 From left: Germany, Berlin and the study area in Central Berlin. *Source*: Data source base maps: SenStadt (2015), SenStadt (2018)

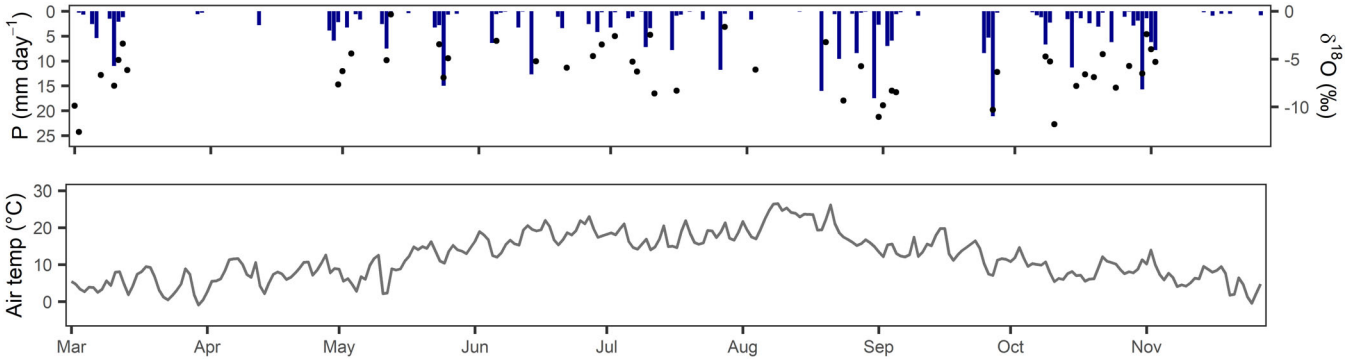

FIGURE 2 Precipitation (P), $\delta^{18}O$ in precipitation and air temperature from March to November 2020

FIGURE 3 $\delta^{18}O$ and $\delta^{2}H$ in precipitation and soil water from March to November 2020. LMWL = local meteoric water line

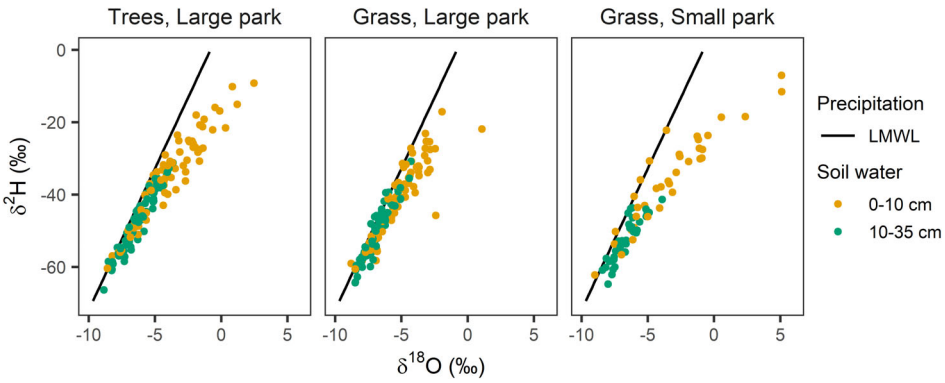

tree plot sites) and in Weinberg (one grass plot site). The measurements were performed multiple days per week between March and November 2020 with data gaps during the second part of June as well as from the end of August until the beginning of November due to equipment failure and delayed repairs during the COVID-19 pandemic. We used a Theta handheld probe ML3 Sensor from Delta-T Devices (Cambridge, England) with an accuracy of 3%. Measured depths were an integration of 0–5 cm and each plot site was probed 4–6 times to account for the spatial heterogeneity.

Soil water extraction for subsequent stable isotope analysis was performed in Humboldthain (two grass and two tree plot sites) and in Weinberg (one grass plot site) and followed the direct water vapour

equilibrium method (Wassenaar et al., 2008, Figure 3). We took duplicate samples per plot site with ~10 m distance. Each sample contained two soil cores in close distance (~15 cm) to obtain the 2–3 ml of bulk soil water needed (Gralher et al., 2021; Hendry et al., 2015). Samples were stored to achieve equilibrium for 48 h in a climate-controlled laboratory (± 0.5°C during measurement). We used aluminium-coated bags which were heat-sealed after introducing artificial dry air. For all samples, including three standards (normalized to VSMOW), the isotopic composition was measured using a Los Gatos Research Integrated Cavity Output Spectroscopy (OA-ICOS) Analyser (LGR, TIWA-45-EP, San Jose, CA, precision: 0.2 and 0.05‰ for δ^2H and $\delta^{18}O$, respectively). For a detailed description of measurements see Marx et al. (in review).

2.3 | Model domain

The green space in the model domain was classified into two vegetation cover types (trees and grass) and two size classes (large and small parks). The category large park was restricted to the biggest park in the model domain Humboldthain, and all other green spaces, including the two parks Brunnenplatz and Weinberg, were categorized as small parks. This was because we expected the larger park to have a different microclimate compared to the smaller green patches and because of the SWC differences observed in the measured data. The model domain was divided into grids with the size 50 × 50 m. Each cell was assigned only one vegetation type, based on aerial photos (SenStadt, 2018, Figure 4). The model domain was reduced by omitting parts of the SW where no calibration data was available to reduce computational time.

Each cell potentially has a sealed area, ranging from 0% to 100% based on the sealed surface map provided by the Berlin Senate (SenStadt, 2017). Based on the digital elevation map (SenStadt, 2021) a local drainage direction was calculated using PCRaster (PCRaster, 2021). Excess water from sealed surfaces runs off following the gravitational flow direction. The model domain drains towards the SW, mimicking artificial urban drainage losses (Figure S1). In total, the model domain comprises 69% sealed surface, 28.5% trees (24% in small parks, 4.5% is the large park) and 2.5% grass (2% small parks, 0.5% large park).

2.4 | Model description

EcH_2O-iso is a process-based, tracer-aided ecohydrological model containing three modules simulating energy balance, hydrology and vegetation dynamics. The original EcH_2O model is described in Maneta and Silverman (2013) and the EcH_2O-iso isotope extension is described in Kuppel et al. (2018), here only a very brief summary follows. The energy balance module consists of the canopy layer, where solar and longwave radiation is used to simulate sensible heat, latent heat and net radiation, and a surface layer where sensible heat, latent heat, net radiation, ground heat flux and latent heat of snowmelt are simulated. The water balance module partitions precipitation by canopy interception and evaporation, ponding on top of the soil, infiltration into the soil (using the Green-Ampt model), soil evaporation, transpiration, recharge as well as surface and groundwater run-on and runoff. The ET components are separately estimated using the energy balance. The soil is conceptualized as three layers; vertical movement is conceptualized using a kinematic approximation when field capacity is exceeded, with lateral flow only possible in the lowest layer or on the soil surface. As we did not focus on gross primary production in this study, we had the vegetation dynamics switched off. The isotope module tracks the stable water isotope (δ^2H and $\delta^{18}O$) composition of the water throughout the compartments and fluxes including evaporative fractionation and mixing between soil layers (see Kuppel et al., 2018 for details).

2.5 | Evaporation from sealed surfaces

We assumed an average interception capacity for the sealed surfaces to be 0.5–1.0 mm. This corresponds to the lower values given in Timm et al. (2018) to account for sloping rooftops, which were assumed to have lower interception. To estimate interception evaporation from sealed surfaces, we used a simple first approximation where:

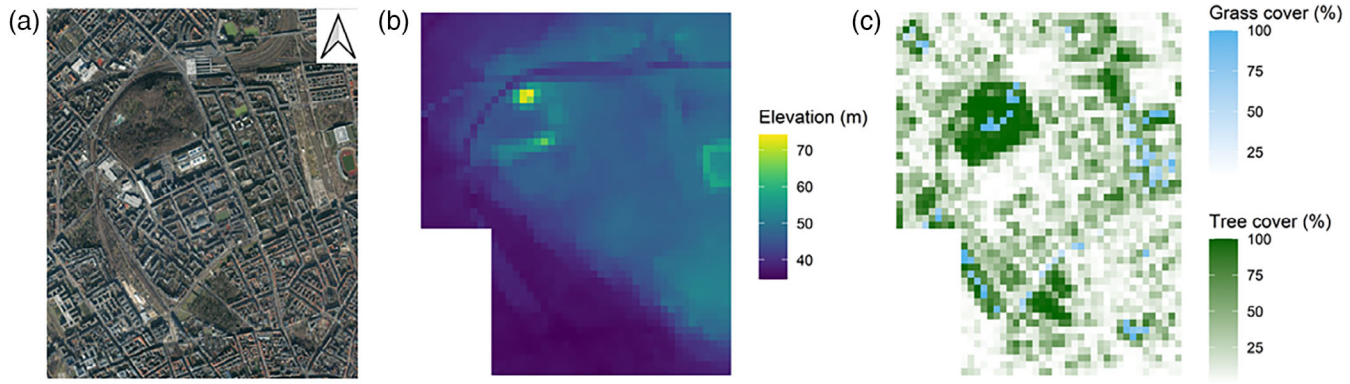

FIGURE 4 Satellite photo (a), digital elevation map (b) and vegetation cover (c) of the model domain. (b) and (c) are in 50 × 50 m resolution and the white area on the lower-left indicates an omitted in the modelling process to shorten the computational time

$$E_{sealed} = \frac{S_{sealed}}{S_{canopy}} * E_{canopy} \quad (1)$$

Where E_{sealed} is the evaporation from sealed surfaces (mm), S_{sealed} is the storage capacity of sealed surfaces (mm), S_{canopy} is the storage capacity of tree canopy (mm) and E_{canopy} is the evaporation from intercepted water by the tree canopy (mm). The S_{canopy} is calculated by multiplying LAI (–) with CWS_{max} (mm)—the maximum storage capacity of the canopy.

To estimate the evapotranspiration over the whole model domain the simulated values were multiplied with the proportion of each land use: trees (large and small park), grass (large and small park) and sealed surface.

2.6 | Calibration and validation

To calibrate the model, we used the Kling-Gupta efficiency (KGE, Gupta et al., 2009) as the objective function. To choose which parameters to vary, a sensitivity analysis following the Morris method (Morris, 1991; Sohier et al., 2014) was performed. The initial parameters were randomized using Latin hypercube sampling (McKay et al., 1979). The sensitivity was evaluated using root-mean-square-error over 100 trajectories. The initial parameter ranges (Table 1) were for the most part similar between trees and grass and the different parks with some exceptions: Leaf Area Index (LAI) was set higher for trees compared with grass and slightly higher for grass in the large park compared with the small parks due to higher recreational usage and trampling in the smaller parks; the exponential root profile was set higher for grass than for trees to distribute the roots at shallower depths for grass.

Multi-criteria calibration was performed using SWC in the top layer and soil water isotopes in the upper two layers. Since there were more SWC data collected compared with soil water isotopes, more weight was given to the SWC data. In an iterative process, sets of 40 000–60 000 Monte Carlo runs were conducted to narrow the parameter ranges. As a final step, a larger set of 150 000 runs was performed and the best 50 runs were used for visualization and calculation of output parameters of interest. Tables S1 and S2 Supplement contain the final calibration ranges and the values of parameters not included in the calibration process.

3 | RESULTS

3.1 | Soil water content

The modelled period was relatively wet, with well-distributed rainfall events through the summer (Figure 2). There was a general switch

TABLE 1 Initial parameter ranges for trees and grass in the small parks and the large park

Parameter	Abbreviation	Calibration range			
Vegetation parameters		**Trees, small park**	**Grass, small parks**	**Trees, large park**	**Grass, large park**
Vegetation albedo (–)	α_{veg}	0.1–0.2	0.1–0.2	0.1–0.2	0.1–0.2
Leaf area index (LAI) (m^2/m^2)	LAI	3.8–5.0	1.5–2.5	3.8–5.0	2.0–3.0
Maximum stomatal conductance (m/s)	gs_{max}	0.0005–0.07	0.0005–0.07	0.0005–0.07	0.0005–0.07
Stomatal sensitivity to vapour pressure deficit (1/Pa)	gs_{vpd}	10^{-5}–10^{-3}	10^{-5}–10^{-3}	10^{-5}–10^{-3}	10^{-5}–10^{-3}
Stomatal sensitivity to light (W/m^2)	gs_{light}	1–500	1–500	1–500	1–500
Stomatal sensitivity to soil moisture content (–)	L_{WPC}	10^{-4}–5×10^{1}	10^{-4}–5×10^{1}	10^{-4}–5×10^{1}	10^{-4}–5×10^{1}
Soil moisture suction potential at which stomatal function is reduced by 50% (m)	L_{WPD}	1–200	1–200	1–200	1–200
Light extinction coefficient for the canopy (–)	K_{beer}	0.2–0.8	0.2–0.8	0.2–0.8	0.2–0.8
Optimal growth temperature (°C)	T_{opt}	10–20	10–20	10–20	10–20
Soil parameters		**Trees, small park**	**Grass, small park**	**Trees, large park**	**Grass, large park**
Total soil depth (m)	D_{soil}	1–7	1–7	1–7	1–7
Thickness of 1st hydrological layer (m)	D_{L1}	0.05–0.15	0.05–0-15	0.05–0.15	0.05–0.15
Thickness of 2nd hydrological layer (m)	D_{L2}	0.3–0.6	0.3–0.6	0.3–0.6	0.3–0.6
Porosity (m^3/m^3)	H	0.35–0.55	0.35–0.55	0.35–0.55	0.35–0.55
Air-entry pressure head (m)	ψ_{AE}	0.15–0.55	0.15–0.55	0.15–0.55	0.15–0.55
Saturated horizontal hydraulic conductivity (m/s)	K_{EFF}	10^{-5}–5×10^{-3}	10^{-5}–5×10^{-3}	10^{-5}–5×10^{-3}	10^{-5}–5×10^{-3}
Exponential root profile (1/m)	k_{root}	0.1–15	5–40	0.1–15	5–40
Brooks-corey exponent (–)	λ_{BC}	2–7	2–7	2–7	2–7
Leakance (–)	L	0.1–0.9	0.1–0.9	0.1–0.9	0.1–0.9

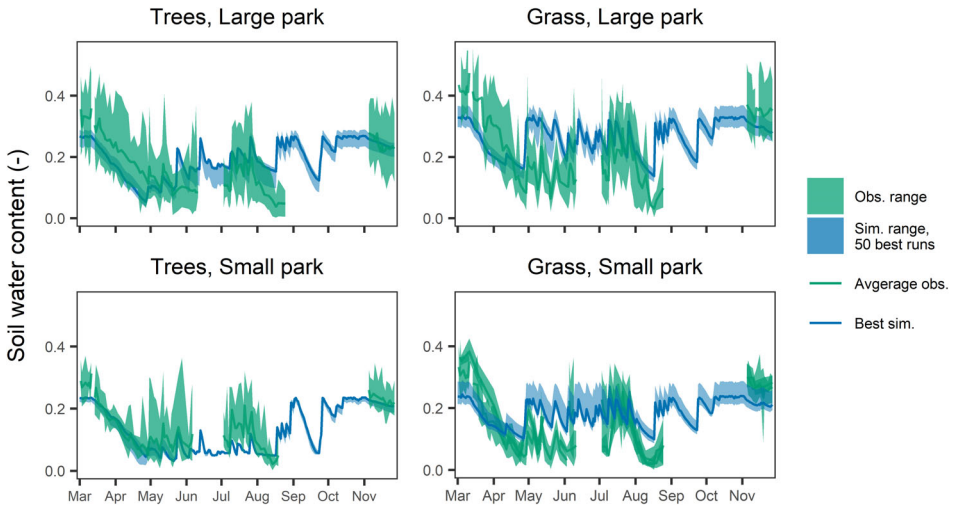

FIGURE 5 Observed (Obs.) and simulated (Sim.) soil water content under trees and grass

from isotopically depleted early spring rainfall in March, to more enriched summer rainfall in June and July, and then back to more depleted rain in the autumn (Figure 2). Despite this general seasonal pattern, variability in the isotopic composition of rainfall between individual events was large.

The fit of SWC in the calibrated model was reasonable for all vegetation types and parks, though better under trees and weaker under grass (Figure 5). Under trees, the simulated values were almost consistently within the measured range, except for a short period in the small park in July, where values were underestimated. Under grass, the model did not track the extreme dynamics, where values changed from <0.05 to >0.3 in only a few days. Consequently, simulations show a more flattened response but follow the measured dynamics, albeit in a damped way. KGE values based on the best multi-criteria run were 0.88 and 0.65 for trees in the large and small park, respectively. Under grass, KGE values were 0.43 in the large park and 0.35 and 0.27 in the small parks.

3.2 | Soil water isotopes

The model also captured the seasonal changes of soil water isotopes under all vegetation types and in both layers in response to rainfall inputs mixing with resident soil water and evaporation effects (Figure 6: $\delta^{18}O$, Figure S2: $\delta^{2}H$). In layer 1 (0–5 cm for grass, 0–15 cm for trees), there was a marked summer enrichment and a depletion during autumn. Under grass, the enrichment was overestimated in the large park, but under trees and in the small park the fit was reasonable. A similar seasonal pattern was found in layer 2 (15–60 cm) under trees which was well simulated, but with some delay. Under grass the depletion during autumn was less pronounced in layer 2 (5–50 cm) and the model captured this well.

3.3 | Quantification of ecohydrological fluxes

Over the study period, the estimated total evapotranspiration was fairly similar for trees in both large and small parks as well as the

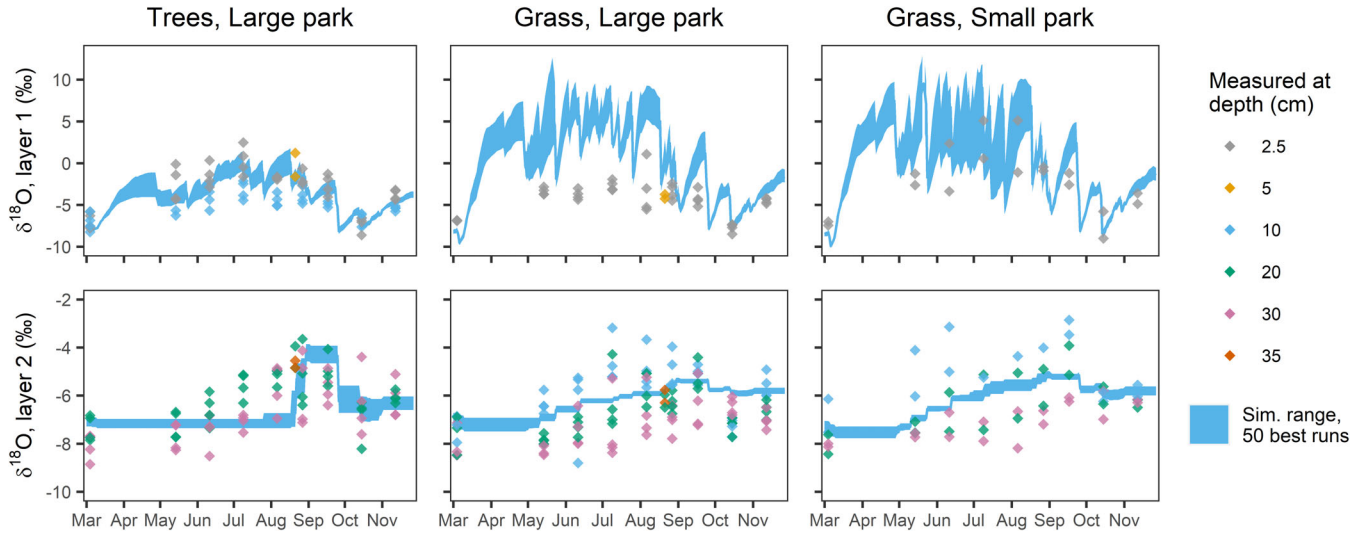

FIGURE 6 Measured and simulated for peer review δ 18O in bulk soil water

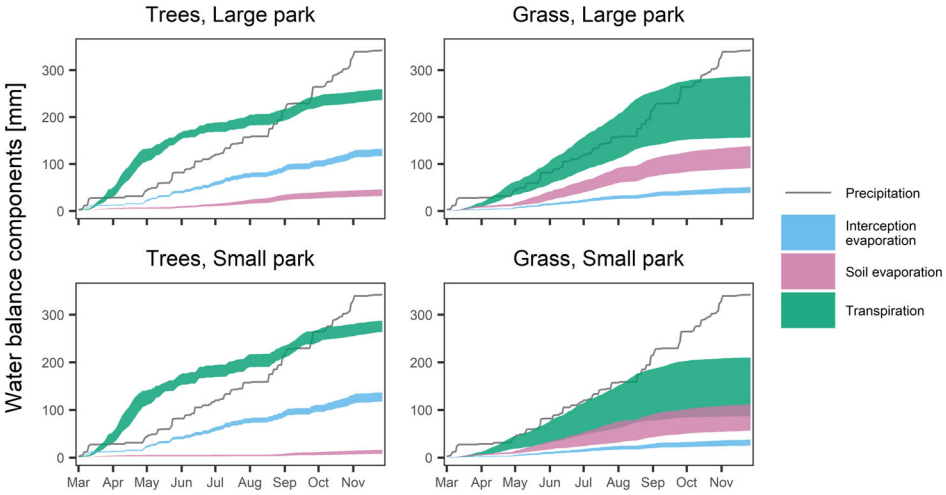

FIGURE 7 Cumulative precipitation, interception evaporation, soil evaporation and transpiration for trees and grass

TABLE 2 Simulated cumulative water balance components transpiration, interception evaporation, soil evaporation, total evapotranspiration (ET), infiltration and recharge

Vegetation type	Transpiration (mm)	Intercept. evap. (mm)	Soil evap. (mm)	Total ET (mm)	Infiltration (mm)	Recharge (mm)
Trees, large park	250 ± 6	125 ± 4	38 ± 3	413 ± 3	217 ± 4	11 ± 2
Trees, small park	278 ± 6	125 ± 5	12 ± 2	415 ± 4	217 ± 5	10 ± 3
Grass, large park	253 ± 39	47 ± 4	105 ± 14	405 ± 29	295 ± 4	89 ± 12
Grass, small park	160 ± 28	33 ± 3	93 ± 11	286 ± 23	279 ± 3	126 ± 8
100% sealed surface	0	36 ± 12	0	36 ± 12	0	0

Note: Mean and *SD* of 50 top runs.

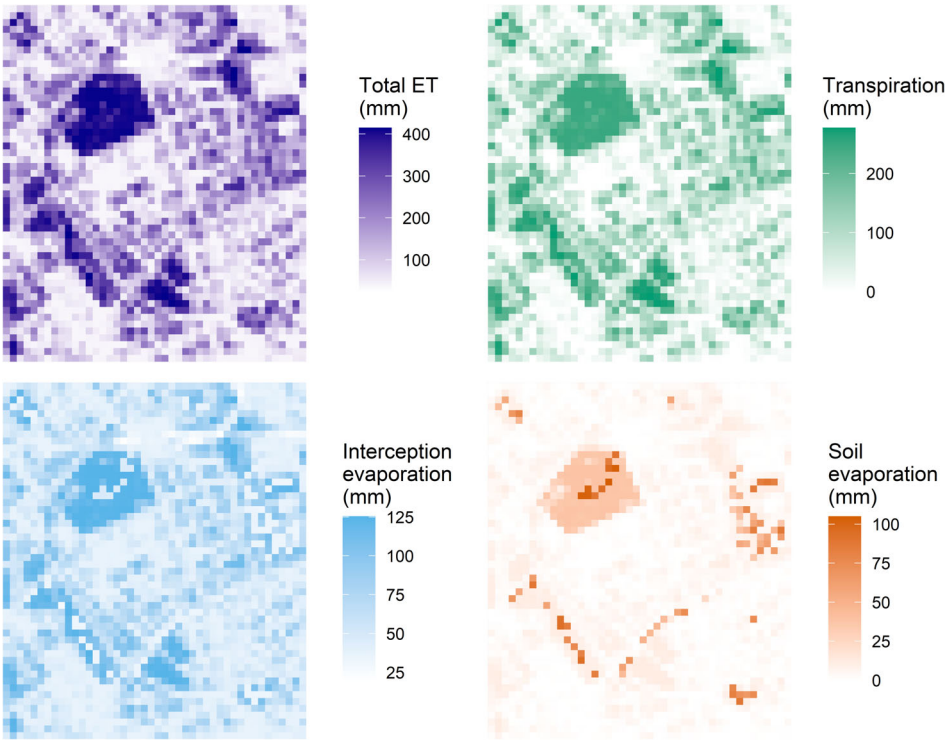

FIGURE 8 Evapotranspiration (ET), transpiration, interception evaporation from vegetation and sealed surfaces, and soil evaporation aggregated over the period March–November 2020

grass in large park, but lower for grass in small parks (Figure 7, Table 2). Transpiration was slightly higher for trees in the small park compared to the large park, while soil evaporation was higher in the large park. For grass, soil evaporation was much higher compared with trees, while interception evaporation was much lower. For grass in the large park, transpiration was close to that of trees but

the uncertainty bounds for transpiration and soil evaporation were much larger. The high evaporation is consistent with the overprediction of soil water isotopes in layer 1 and implies an overestimate of evaporative fluxes (Figure 6). Transpiration was lower for grass in the small parks compared to both trees as well as grass in the large park.

The cumulative ecohydrological fluxes over the whole model area for the study period reveal the spatial influence of vegetation (Figure 8). The large park and green patches provide sources of high evaporation fluxes while the sealed surfaces contribute very little. The difference between trees and grass was also clear with higher soil evaporation from grass and higher transpiration from trees. For the whole model domain, the estimated sum of evapotranspiration from trees (which cover 28.5% of the area) was 78% of the total evapotranspiration, while only 5% was from grass and 17% from sealed surfaces.

As a consequence of the greater evapotranspiration from the trees, estimated summer recharge under patches of grassland increases during the modelled period by a factor of 8 and 12 for small and large parks respectively. These differences are likely lower over the whole year, when winter recharge under trees will be greater, but do highlight the potential effects of increased green water fluxes on residual blue water fluxes.

4 | DISCUSSION

This timely 'proof of concept' exploration showed that the EcH$_2$O-iso model is potentially a useful process-based tool for simulating water fluxes in complex urban landscapes with a varying mosaic of urban green space. However, some limitations immediately also become apparent. In general, the fit of both SWC and soil water stable isotopes was reasonable and showed the utility of even a skeletal programme of soil moisture and the value of soil water isotopes for model calibration. Most mismatches between measurements and simulations reflect the contrast in scale between the averages for modelled soil layers and point measurements, especially for soil moisture. The model most notably overestimated the enrichment of soil water stable isotopes from evaporative fractionation in the upper soil layer in the large park. Here, the model probably failed to represent the more shaded conditions from the trees on elevated land surrounding the grassland (Figure 4). This likely overestimated soil evaporation in the large park given the relatively high SWC, though this error was quite modest in relation to the overall ET flux in the model domain which was dominated by trees. However, in general large parks are also likely to have their own microclimates, being cooler and more humid from shading and latent heat transfers (Bowler et al., 2010). This likely also contributed to the uncertainty over transpiration estimates here as well, especially the parameter sets which simulated higher rates.

Compared with the results in Gillefalk et al. (2021) the SWC values used in this study were much more dynamic and sensitive, most probably because the measurements were carried out at 0–5 cm depth compared with more damped responses at 10–15 cm depth in the previous study. Furthermore, as the simulation in this study used daily timesteps, capturing instantaneous point measurements was more challenging and sudden peaks were harder to reproduce, as seen for example in July and August (Figure 5). Nevertheless, given the critical importance of the soil surface to water partitioning, even such shallow soil moisture data has a powerful information content for model calibration. For a more comprehensive calibration, however, intense data collection with high resolution in both space and time, including deeper soil horizons, is needed, something that is difficult in urban areas due to high heterogeneity, accessibility, the need for permits and risk of vandalism. An alternative to direct measurements would be to use remote sensing data, which in turn has its own challenges: getting permits to fly an unmanned aerial vehicle (drone) over urban areas is very complicated and satellite images are either low resolution or very expensive. Overcoming these challenges is crucial as the study has highlighted the importance of microclimate, for example affecting evaporation estimates in larger parks like Humboldthain, which would need to be more thoroughly assessed through high-resolution monitoring. In addition, further work is needed into more generic scaling effects in complex urban landscapes, as well as edge effects and variable sized parcels of land (e.g., Ichiba et al., 2018). Finally, there is still high uncertainty in our approach regarding evaporation from impermeable surfaces and our estimates are likely on the conservative side. A differentiation, at least between tilted rooftops and other sealed surfaces, would be needed to decrease uncertainty. A related area of improvement is the heat radiation from sealed surfaces. As of now, the model could differentiate between grass and trees, where soil surface temperatures under grass were higher than under trees. However, the model was not yet fit to calculate temperatures of sealed surfaces, which were shown to be similar to grass-covered areas.

Trees in general used more water than grass in the study year, primarily due to higher interception, but also higher transpiration. The difference was largest in the small parks. However, model uncertainty for grass in the large park was high, probably reflecting the model struggling to converge solutions for simulations of soil moisture and soil water isotopes and a wide range of some parameters. This likely reflects the shading effects of surrounding trees, which resulted in higher soil moisture which the model could utilize to sustain high soil evaporation and transpiration, as driving radiation was higher than in reality. Nevertheless, interception evaporation and transpiration from trees were the dominant components of the ET flux from the model domain. This generalizes the results of Gillefalk et al. (2021) and highlights the importance of urban trees, especially in contiguous stands or forests, as dominant sources of water flux that would help mitigate the urban heat island effect. In turn, the importance for urban trees to have access to deeper soil water and/or groundwater has been shown by Marchionni et al. (2019). The dry years of 2018 and 2019 created water limitations for trees (Gillefalk et al., 2021; Kuhlemann et al., 2021), and with ongoing climate change, the vulnerability for trees can be expected to increase. It is therefore important to choose the right combination of species for a particular location, for example,

the right integration of trees and turf grass can optimize the cooling effect while lowering irrigation needs (Gómez-Navarro et al., 2021).

This study serves as a stepping stone for further work using isotopes to help upscaling green flux modelling in complex urban settings and shows the value of distributed, near-surface SWC measurements. The extended soil moisture measurement program by the Berlin senate department for the environment, transport and climate protection set into place at the end of 2020 has the potential in aiding future upscaling modelling projects as well as giving crucial guidance for irrigation. In order to further increase the possibility of high-resolution measurement campaigns, citizen science projects come to mind. Stable water isotope data from soil or xylem can also be used to not only estimate sources of root water uptake under different vegetation types but also to estimate water ages in different stores and fluxes (Smith et al., 2021). Similar to our earlier work (Gillefalk et al., 2021), in the current application, EcH$_2$O-iso estimated that the mean age of soil water in layers 1 and 2 was in the order of ~2 weeks and ~ 5 months, respectively under both grass and trees (Table S3). However, in layer 3 (at a depth of >0.5 m) the age increased to ~18 months and 24 months in grass and trees, respectively (Table S3), indicating the greater recharge under grass. This information can in turn inform on response times of vegetation to precipitation events and drought recovery—which will generally be longer for trees—as well as resilient adaptation strategies used by trees during prolonged periods of drought.

5 | CONCLUSION

Tracer-aided ecohydrological models have considerable potential for constraining estimates of ecohydrological partitioning in large-scale, complex urban landscapes. With adequate driving data, even limited soil moisture and soil water isotope data can act as useful calibration constraints. The application, here for ~5 km^2 of the city of Berlin, shows the importance of urban trees, particularly in contiguous stands in parks and urban forests, as the dominant source of urban evapotranspiration, with around 80% of the total coming from 30% of the area. To advance urban ecohydrological modelling, more detailed field data collection is needed and assessment of the utility of remote sensing products. In addition, adaptations of model structures are required to conceptualize important urban effects (e.g., shading, heat retention in building etc.).

ACKNOWLEDGEMENTS

The authors wish to thank the Einstein Foundation Berlin for financing the MOSAIC project (EVF-2018-425), in which this study was performed. MG and CM are associated with the Research Training Group 'Urban Water Interfaces' (UWI), GRK 2032/2 as collegiates. Contributions from CS were also funded by the Leverhulme Trust's ISOLAND project. Funding was also received through the Einstein Research Unit 'Climate and Water under Change' from the Einstein Foundation Berlin and Berlin University Alliance. The German Federal Ministry of Education and Research (BMBF) funded instrumentation of the Urban Climate Observatory (UCO) Berlin under grant 01LP1602 within the framework of Research for Sustainable Development (FONA; www.fona.de). The simulations were performed on the High Performance Computing cluster of TU Berlin. We acknowledge support by the German Research Foundation and the Open Access Publication Fund of TU Berlin.

DATA AVAILABILITY STATEMENT

Precipitation isotopes and data on soil water content are available upon reasonable request. Precipitation data are available publicly from the Deutsche Wetterdienst (DWD). Digital elevation map, aerial phots, land use data and sealed surface data are publicly available from the Berlin Senate.

ORCID

Mikael Gillefalk https://orcid.org/0000-0002-7642-776X
Doerthe Tetzlaff https://orcid.org/0000-0002-7183-8674
Christian Marx https://orcid.org/0000-0001-7648-1603
Aaron Smith https://orcid.org/0000-0002-2763-1182
Fred Meier https://orcid.org/0000-0003-0399-2757
Chris Soulsby https://orcid.org/0000-0001-6910-2118

REFERENCES

Beck, H. E., Zimmermann, N. E., McVicar, T. R., Vergopolan, N., Berg, A., & Wood, E. F. (2018). Present and future Köppen-Geiger climate classification maps at 1-km resolution. *Scientific Data*, *5*(1), 180214. https://doi.org/10.1038/sdata.2018.214

Bowler, D. E., Buyung-Ali, L., Knight, T. M., & Pullin, A. S. (2010). Urban greening to cool towns and cities: A systematic review of the empirical evidence. *Landscape and Urban Planning*, *97*(3), 147–155. https://doi.org/10.1016/j.landurbplan.2010.05.006

Cao, X., Lyu, H., Ni, G., Tian, F., Ma, Y., & Grimmond, C. S. B. (2020). Spatial scale effect of surface routing and its parameter Upscaling for urban flood simulation using a grid-based model. *Water Resources Research*, *56*(2), e2019WR025468. https://doi.org/10.1029/2019WR025468

Cristiano, E., Deidda, R., & Viola, F. (2020). EHSMu: A new Ecohydrological Streamflow model to estimate runoff in urban areas. *Water Resources Management*, *34*(15), 4865–4879. https://doi.org/10.1007/s11269-020-02696-0

Deutscher Wetterdienst (DWD). 2020. Vieljährige Mittelwerte Available at: https://www.dwd.de/DE/leistungen/klimadatendeutschland/vielj_mittelwerte.html.

Ehleringer, J. R., Barnette, J. E., Jameel, Y., Tipple, B. J., & Bowen, G. J. (2016). Urban water – A new frontier in isotope hydrology. *Isotopes in Environmental and Health Studies*, *52*(4–5), 477–486. https://doi.org/10.1080/10256016.2016.1171217

Gillefalk, M., Tetzlaff, D., Hinkelmann, R., Kuhlemann, L.-M., Smith, A., Meier, F., Maneta, M. P., & Soulsby, C. (2021). Quantifying the effects of urban green space on water partitioning and ages using an isotope-based ecohydrological model. *Hydrology and Earth System Sciences*, *25*(6), 3635–3652. https://doi.org/10.5194/hess-25-3635-2021

Golden, H. E., & Hoghooghi, N. (2018). Green infrastructure and its catchment-scale effects: An emerging science. *WIREs Water*, *5*(1), e1254. https://doi.org/10.1002/wat2.1254

Gómez-Navarro, C., Pataki, D. E., Pardyjak, E. R., & Bowling, D. R. (2021). Effects of vegetation on the spatial and temporal variation of microclimate in the urbanized salt Lake Valley. *Agricultural and Forest Meteorology*, *296*, 108211. https://doi.org/10.1016/j.agrformet.2020.108211

Gralher, B., Herbstritt, B., & Weiler, M. (2021). Technical note: Unresolved aspects of the direct vapor equilibration method for stable isotope analysis (δ18O, δ2H) of matrix-bound water: Unifying protocols through empirical and mathematical scrutiny. *Hydrology and Earth System Sciences*, *25*(9), 5219–5235. https://doi.org/10.5194/hess-25-5219-2021

Gupta, H. V., Kling, H., Yilmaz, K. K., & Martinez, G. F. (2009). Decomposition of the mean squared error and NSE performance criteria: Implications for improving hydrological modelling. *Journal of Hydrology*, *377*(1), 80–91. https://doi.org/10.1016/j.jhydrol.2009.08.003

Hendry, M. J., Schmeling, E., Wassenaar, L. I., Barbour, S. L., & Pratt, D. (2015). Determining the stable isotope composition of pore water from saturated and unsaturated zone core: Improvements to the direct vapour equilibration laser spectrometry method. *Hydrology and Earth System Sciences*, *19*(11), 4427–4440. https://doi.org/10.5194/hess-19-4427-2015

Ichiba, A., Gires, A., Tchiguirinskaia, I., Schertzer, D., Bompard, P., & Ten Veldhuis, M.-C. (2018). Scale effect challenges in urban hydrology highlighted with a distributed hydrological model. *Hydrology and Earth System Sciences*, *22*(1), 331–350. https://doi.org/10.5194/hess-22-331-2018

Kuhlemann, L.-M., Tetzlaff, D., Smith, A., Kleinschmit, B., & Soulsby, C. (2021). Using soil water isotopes to infer the influence of contrasting urban green space on ecohydrological partitioning. *Hydrology and Earth System Sciences*, *25*(2), 927–943. https://doi.org/10.5194/hess-25-927-2021

Kuppel, S., Tetzlaff, D., Maneta, M. P., & Soulsby, C. (2018). EcH2O-iso 1.0: Water isotopes and age tracking in a process-based, distributed ecohydrological model. *Geoscientific Model Development*, *11*(7), 3045–3069. https://doi.org/10.5194/gmd-11-3045-2018

Maneta, M. P., & Silverman, N. L. (2013). A spatially distributed model to simulate water, energy, and vegetation dynamics using information from regional climate models. *Earth Interactions*, *17*(11), 1–44. https://doi.org/10.1175/2012EI000472.1

Marchionni, V., Guyot, A., Tapper, N., Walker, J. P., & Daly, E. (2019). Water balance and tree water use dynamics in remnant urban reserves. *Journal of Hydrology*, *575*, 343–353. https://doi.org/10.1016/j.jhydrol.2019.05.022

Marx, C., Tetzlaff, D., Hinkelmann, R., & Soulsby, C. (in review). Spatial variations in soil-plant interactions in contrasting urban green spaces: Preliminary insights from water stable isotopes. *Journal of Hydrology*.

McKay, M. D., Beckman, R. J., & Conover, W. J. (1979). A comparison of three methods for selecting values of input variables in the analysis of output from a computer code. *Technometrics*, *21*(2), 239–245. https://doi.org/10.2307/1268522

Meili, N., Manoli, G., Burlando, P., Bou-Zeid, E., Chow, W. T. L., Coutts, A. M., Daly, E., Nice, K. A., Roth, M., Tapper, N. J., Velasco, E., Vivoni, E. R., & Fatichi, S. (2020). An urban ecohydrological model to quantify the effect of vegetation on urban climate and hydrology (UT&C v1.0). *Geoscientific Model Development*, *13*(1), 335–362. https://doi.org/10.5194/gmd-13-335-2020

Morris, M. D. (1991). Factorial sampling plans for preliminary computational experiments. *Technometrics*, *33*(2), 161–174. https://doi.org/10.2307/1269043

PCRaster documentation. 2021 Available at: https://pcraster.geo.uu.nl/pcraster/4.3.1/documentation/pcraster_manual/sphinx/op_lddcreate.html

Peng, S., Piao, S., Ciais, P., Friedlingstein, P., Ottle, C., Bréon, F.-M., Nan, H., Zhou, L., & Myneni, R. B. (2012). Surface urban heat Island across 419 global big cities. *Environmental Science & Technology*, *46*(2), 696–703. https://doi.org/10.1021/es2030438

Senate Department for Urban Development (SenStadt). 2015. Umweltatlas Berlin / Reale Nutzung der bebauten Flächen. Available at: https://fbinter.stadt-berlin.de/fb/index.jsp?loginkey=showMap&mapId=realnutz2015@senstadt

Senate Department for Urban Development (SenStadt). 2017. Umweltatlas Berlin / Versiegelung. Data license Germany - attribution - Version 2.0. Available at: https://www.stadtentwicklung.berlin.de/umwelt/umweltatlas/e_text/kd102.pdf

Senate Department for Urban Development (SenStadt). 2018. Digitale farbige Orthophotos 2018 (DOP20RGB) Available at: https://fbinter.stadt-berlin.de/fb/berlin/service_intern.jsp?id=a_luftbild2018_rgb@senstadt&type=FEED

Senate Department for Urban Development (SenStadt). 2021. ATKIS DGM - Digitales Geländemodell. Data license Germany - attribution - Version 2.0. Available at: https://www.stadtentwicklung.berlin.de/geoinformation/landesvermessung/atkis/de/dgm.shtml

Smith, A., Tetzlaff, D., Kleine, L., Maneta, M., & Soulsby, C. (2021). Quantifying the effects of land use and model scale on water partitioning and water ages using tracer-aided ecohydrological models. *Hydrology and Earth System Sciences*, *25*(4), 2239–2259. https://doi.org/10.5194/hess-25-2239-2021

Sohier, H., Farges, J.-L., & Piet-Lahanier, H. (2014). Improvement of the representativity of the Morris method for air-launch-to-orbit separation. *IFAC Proceedings Volumes*, *47*(3), 7954–7959. https://doi.org/10.3182/20140824-6-ZA-1003.01968

Tague, C. L., Papuga, S. A., Gerlein-Safdi, C., Dymond, S., Morrison, R. R., Boyer, E. W., Riveros-Iregui, D., Agee, E., Arora, B., Dialynas, Y. G., Hansen, A., Krause, S., Kuppel, S., Loheide, S. P., II, Schymanski, S. J., & Zipper, S. C. (2020). Adding our leaves: A community-wide perspective on research directions in ecohydrology. *Hydrological Processes*, *34*(7), 1665–1673. https://doi.org/10.1002/hyp.13693

Timm, A., Kluge, B., & Wessolek, G. (2018). Hydrological balance of paved surfaces in moist mid-latitude climate – A review. *Landscape and Urban Planning*, *175*, 80–91. https://doi.org/10.1016/j.landurbplan.2018.03.014

Wassenaar, L. I., Hendry, M. J., Chostner, V. L., & Lis, G. P. (2008). High resolution pore water δ2H and δ18O measurements by H2O(liquid)–H2O(vapor) equilibration laser spectroscopy. *Environmental Science & Technology*, *42*(24), 9262–9267. https://doi.org/10.1021/es802065s

Zhou, Z., Smith, J. A., Yang, L., Baeck, M. L., Chaney, M., Ten Veldhuis, M.-C., Deng, H., & Liu, S. (2017). The complexities of urban flood response: Flood frequency analyses for the Charlotte metropolitan region. *Water Resources Research*, *53*(8), 7401–7425. https://doi.org/10.1002/2016WR019997

SUPPORTING INFORMATION

Additional supporting information may be found in the online version of the article at the publisher's website.

How to cite this article: Gillefalk, M., Tetzlaff, D., Marx, C., Smith, A., Meier, F., Hinkelmann, R., & Soulsby, C. (2022). Estimates of water partitioning in complex urban landscapes with isotope-aided ecohydrological modelling. *Hydrological Processes*, *36*(3), e14532. https://doi.org/10.1002/hyp.14532